

## A simple 3D plasma instrument with an electrically adjustable geometric factor for space research

This article has been downloaded from IOPscience. Please scroll down to see the full text article.

2012 Meas. Sci. Technol. 23 025901

(<http://iopscience.iop.org/0957-0233/23/2/025901>)

View [the table of contents for this issue](#), or go to the [journal homepage](#) for more

Download details:

IP Address: 80.219.44.195

The article was downloaded on 06/01/2012 at 05:14

Please note that [terms and conditions apply](#).

# A simple 3D plasma instrument with an electrically adjustable geometric factor for space research

U Rohner<sup>1,5</sup>, L Saul<sup>2</sup>, P Wurz<sup>2</sup>, F Allegrini<sup>3,4</sup>, J Scheer<sup>2</sup> and D McComas<sup>3,4</sup>

<sup>1</sup> TOFWERK AG, Uttigenstrasse 22, CH-3600 Thun, Switzerland

<sup>2</sup> Physikalisches Institut, Universität Bern, Sidlerstrasse 5, CH-3012 Bern, Switzerland

<sup>3</sup> Southwest Research Institute, San Antonio, TX 78228-0510, USA

<sup>4</sup> University of Texas at San Antonio, San Antonio, TX 78249, USA

E-mail: [rohner@tofwerk.com](mailto:rohner@tofwerk.com)

Received 16 July 2011, in final form 28 October 2011

Published 5 January 2012

Online at [stacks.iop.org/MST/23/025901](http://stacks.iop.org/MST/23/025901)

## Abstract

We report on the design and experimental verification of a novel charged particle detector and an energy spectrometer with variable geometric factor functionality. Charged particle populations in the inner heliosphere create fluxes that can vary over many orders of magnitude in flux intensity. Space missions that plan to observe plasma fluxes, for example when travelling close to the Sun or to a planetary magnetosphere, require rapid particle measurements over the full three-dimensional velocity distribution. Traditionally, such measurements are carried out with plasma instrumentation with a fixed geometrical factor, which can only operate in a limited range of flux intensity. Here we report on the design and testing of a prototype sensor, which is capable of measuring particle flux with high angular and energy resolution, yet has a variable geometric factor that is controlled without moving parts. This prototype was designed in support of a proposal to make fast electron measurements on the Solar Probe Plus (SP+) mission planned by NASA. We simulated the ion optics inside the instrument and optimized the performance to design and build our prototype. This prototype was then tested in the MEFISTO facility at the University of Bern and its performance was verified over the full range of azimuth, elevation, energy and intensity.

**Keywords:** plasma instrument, space instrumentation, 3D particle imaging, variable geometric factor

(Some figures in this article are in colour only in the electronic version)

## 1. Introduction

The characterization of plasmas in the space environment (e.g. magnetospheric or solar wind plasmas) is a demanding endeavour. Usually three-dimensional velocity distribution functions over a large energy range are required, often together with high time resolution because space plasmas can exhibit rapid fluctuations. This results in the need for plasma

instrumentation with a high dynamic range, often requiring six decades and more of dynamic range. The parameter space for ion measurements in space plasmas has been summarized by Lin *et al* (1995) and Rème *et al* (1997) and covers the energy range from eV to tens of keV, and intensities spanning seven decades. Similarly, the parameter space for electrons covers the energy range from eV to tens of keV, and intensities spanning nine decades, as has been reviewed by Lin *et al* (1995). Electrons are important both because they are current carriers and support many of the various wave modes in the plasma. Thus, higher temporal resolution in

<sup>5</sup> Author to whom any correspondence should be addressed.

the electron measurement is often needed when studying space plasmas, which necessitates a high dynamic range during a short integration time.

Particle energies and incident angles are typically scanned to obtain 3D distribution functions. For most electrostatic analyser-based instruments, the particle energy and the elevation angle are scanned, and the azimuth angle of the registered particle is imaged. Thus, the geometric factor of the instrument is chosen such that the detector does not saturate when measuring at the maximum of the distribution function (see Wurz *et al* 2007). The dynamic range is then given by the capabilities of the actual detector and the integration time. By increasing the integration time one can increase the dynamic range at the expense of time resolution. For ion measurements a compromise along these lines can often be found. For electrons, however, the integration time is often dictated by the frequencies of waves to be studied in the electron plasma. Thus, a compromise between steps needed for the energy and angular scan, and an optimized dynamic range of the detector are needed. Sometimes this is not enough and the geometric factor itself has to be changed during the measurement.

A recent example for very demanding plasma instrumentation came out of the definition of the Solar Probe Plus (SP+) mission planned by NASA (McComas *et al* 2007, 2008). For both the ion and the electron measurement the requirements from the science investigation ask for improved instrument capabilities compared to present state-of-the-art plasma instrumentation. Since the electron measurement is the most ambitious in terms of the instrument capabilities we will focus on this measurement. The requirements from the SP+ mission definition are as follows: (i) a dynamic range adequate to measure 2D distributions in 0.1 s, 3D distributions in 3 s, (ii) an energy range of 1 eV to 5 keV with an energy resolution of  $\Delta E/E = 0.1$ , (iii) angular resolution of  $3^\circ$ , at least in one dimension and (iv) as much of full sky coverage as possible. Being accommodated on a spacecraft, at least two instruments are necessary to provide the full sky coverage. This set of requirements is even more challenging in view of the orbit of the spacecraft spanning from  $140 R_S$  down to  $9.5 R_S$  (solar radii), since average plasma densities scale with distance to the Sun proportional to  $R_S^2$ , which gives a variation in the average flux of over 200. A similar set of requirements for ESA's Solar Orbiter mission has also led to development of a variable geometric factor device for the Solar wind analyser/Electron analyser system.

In addition to challenging measurement requirements, spacecraft resources such as mass, power and others are typically very limited, especially in the case of the SP+ mission, necessitating a simple instrument design. Simple in this case means that the number of high-voltage power supplies is as small as possible, the instrument is compact and the complexity of the detector and the associated electronics is moderate. For the electron measurements of SP+, an instrument to fulfil the requirements needs have to have a variable geometric factor. In the following we present the fast electron analyser (FEA), an instrument we designed specifically for SP+ electron measurements, but of course the basic technology developed can also be used for plasma ion measurements as well.

## 2. Electro-optical design

A popular instrument for space research to derive 3D plasma distribution functions is a plasma analyser based on spherical or toroidal condensers, which have been used in space plasma research for a long time (e.g. Bame *et al* 1967). Carlson *et al* (1983) introduced the  $360^\circ$  angle imaging top hat electrostatic analyser which is still widely used in space plasma research. Although there is a long standing recognition of the need for a large dynamic range in plasma measurements, there are only a few realizations of plasma instruments with a variable geometrical factor. A straightforward approach is to use separate instrument entrances with a different geometric factor. Although having separate entrances with high and low geometric factor works well, it requires more electrodes and thus more power supplies to realize different geometric factors. Since we had to find a solution with low instrument mass, the approach with separate entrances is not feasible in our case. Alternatively, changing the potentials on the different electrodes of the electro-/ion-optical system will change the transmission and thus the geometric factor of the instrument by electronic means. Sauvaud *et al* (2008) presented a design for the electron instrument on *STEREO* where they adjusted the outer and inner potentials of the electrostatic analyser to reduce the geometric factor from its nominal value. With this arrangement they could realize a dynamic range of  $10^8$  in a 2 s measurement. For the *Mercury Magnetospheric Orbiter* spacecraft of the BepiColombo mission, Sauvaud *et al* (2010) developed a concept with a split inner hemisphere (actually a toroid) to adjust the geometric factor, which has the advantage that the outer hemisphere is at ground potential and thus can serve as instrument enclosure at the same time. Also this design allows changing the geometric factor by more than two decades by electronic means. See Collinson and Kataria (2010) for a comparison of different techniques for achieving a variable geometric factor in a top-hat electrostatic analyser.

We decided for a different design for our proposed SP+ instrument because we had to minimize the mass as much as possible. In addition, the requirement of high angular resolution had to be satisfied for at least one angular dimension. The total list of instrument requirements that were working to for this proposal is given in table 1. From the mass and power budget shown in table 1, we decided to build a single entrance ESA in a half-sphere shape. Figure 1 shows a cut through the SIMION 3D model in a late stage of the geometry optimization, close to the built prototype. Elevation scanning is done with two small, toroidal rings placed symmetrically around the entrance slit (denoted as El. up/down). A grid in front of these two electrodes makes a well-defined potential interface to the outside world. Energy scanning is performed by varying the voltage on the half-sphere with radius  $R1$ . The half-sphere is cut in distance  $D1$  from its top, in a distance  $D2$  to the detector front.  $R2$  is the radius of the (grounded) outer shell. The top-plate that sets the basic geometric factor of the instrument is placed in a distance  $D3$  from the inner shell.

The SIMION model of this prototype is fully parametrized, so we applied an iterative two-step optimization strategy already successfully used in the design of the LMS

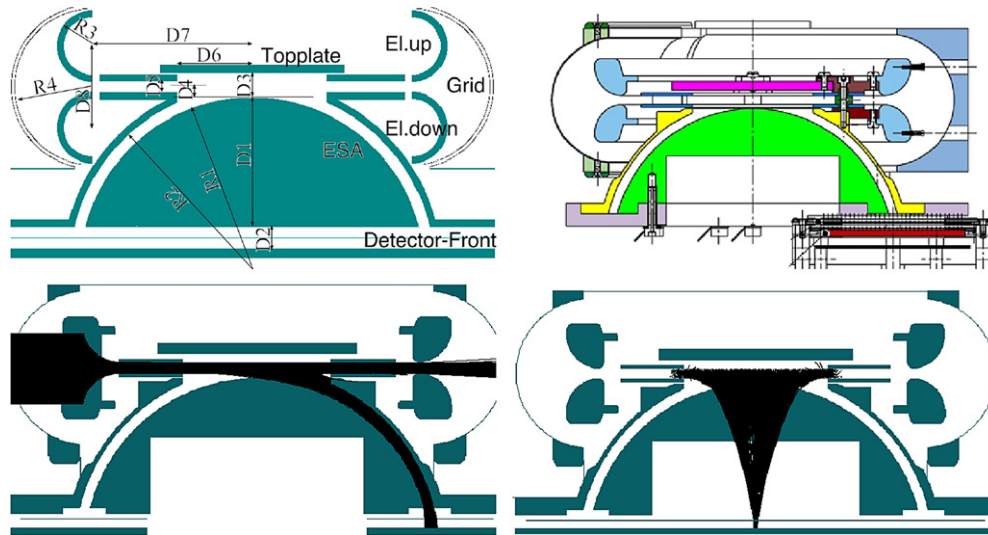


**Figure 1.** Top left: cut through the 3D SIMION geometry with the 12 geometry optimization parameters. Top right: geometry of the prototype with the laboratory position sensitive detector on the lower right. Bottom: trajectories of the final prototype geometry with particles coming from the left, respectively from the back, being detected at the bottom.

**Table 1.** FEA characteristics and performance summary.

Fast electron analyser	Two deflecting top-hat electrostatic	
<b>Mass</b> 4.0 kg $\pm$ 25%	<b>Power</b> 3.6 W	<b>Data rate</b> 18 kbps
Analysers type	Top-hat electron analyser with deflection electrodes at entrance	
Detector type	3 MCPs, Z-stack configuration, extended dynamic range	
Anode type	1D delay line anode system for azimuth angle measurement	
TOF measurement	$\geq 10^6$ events $s^{-1}$ for delay line angle measurements	
<b>Parameter</b>	<b>Requirement</b>	<b>Capability</b>
Particle species	Electrons	Electrons
Sensitivity	2D in 0.1 s @ 20 $R_S$ 3D in 3 s @ 20 $R_S$	2D in 0.1 s @ 20 $R_S$ 3D in 3 s @ 20 $R_S$
Dynamic range	Requires sensitivity and dynamic range adequate to measure 2D distributions in 0.1 s at 20 $R_S$ without saturating the detectors	$10^6$ over energy range during 0.1 s scan (2D). $10^8$ over energy range during 3 s scan (3D).
Geometric factor (incl. efficiencies)		$(0.022\text{--}2.2) \times 10^{-3}$ (cm <sup>2</sup> sr eV eV <sup>-1</sup> )
Spectral range	1 eV–5 keV	1 eV–5 keV in 64 energy steps
Spectral resolution $\Delta E/E$	0.1	0.09 (purely electro-optics)
Field of view		$90^\circ \times 360^\circ$ per FEA unit
Angular range	As much of $4\pi$ sr as possible	$4\pi$ sr with obstructions
Angular resolution	$3^\circ$ (at least 1D, near strahl)	Azimuth: 1–2 $^\circ$ electro-optics, 1 $^\circ$ anode system; total $< 3^\circ$
Temporal resolution	$30^\circ \times 30^\circ$ (elsewhere) 3 s for 3D 0.1 s for 2D (energy–azimuth)	Elevation: $3^\circ$ 3 s for 3D 0.1 s for 2D (energy–azimuth)

instrument (Rohner *et al* 2004) and partially in the PLASTIC instrument (Galvin *et al* 2008). The geometry is represented with 12 independent parameters (with some obvious boundary conditions, see figure 1). From initial dimension estimates, the 12 parameters were set and a SIMION geometry is synthesized. For this start geometry, the potentials for all the electrodes are optimized using a simplex algorithm (there were initially seven electrodes with different potentials). This voltage optimization

algorithm minimizes a scalar objective function  $z$ , which we choose as

$$z = 1 + s_{az} * a + s_{ke} * b - tr * c$$

with  $s_{az}$  being the standard deviation of the spot size on the detector in the azimuthal direction (defines the azimuthal resolution),  $s_{ke}$  the standard deviation of the energy distribution of the splatted test electrons (defines the energy resolution of the ESA),  $tr$  the transmission from

entrance to the detector (defines the geometric factor) and  $a$ ,  $b$ ,  $c$  weighting factors. This objective function is evaluated by flying an adequate number of test particles, typically  $\sim 10^4$  per run, to obtain reasonable statistics. The test particles' start parameters are randomly distributed in space, direction and energy within a reasonable parameter space that is defined by the current test geometry of the instrument. These particles are then flown and those hitting the detector were statistically evaluated. Typically after some hundred SIMION simulations (particle flights), the voltage sets converge, and the test geometry is assessed with the same value of the objective function  $z$ . A new test geometry is then automatically synthesized and the voltages are automatically optimized again for the new geometry and so on. This loop is performed until the best geometry with the smallest  $z$  is found. The geometry optimization routine was also a simplex, with some 'soft' boundaries letting the routine prefer smaller and therefore lighter geometries and (with a smaller weighting factor) also smaller voltages.

During the simulations, we found that it was possible to reduce the number of individually biased electrodes to only four: ESA (inner shell), top plate, detector and alternating one of the two elevation rings, keeping the other electrodes at ground potential. The shape of the top plate is known to be critical, but the simulations and later on also the experiments showed that for carefully chosen distances  $D3$  and  $D6$  a simple flat plate can fulfil its purpose.

To increase the detector lifetime, the voltage setting of the detector front and the grid in between the ESA and the detector can be adjusted to either focus the incoming particles onto a smaller area, which increases the S/N ratio (see below), or for high fluxes to spread them out onto a larger area. Both settings result only a slight degradation of azimuthal resolution.

### 3. Experimental verification

The FEA prototype (figure 2) was tested in the MEFISTO laboratory at the University of Bern. The facility consists of a vacuum chamber and ion beam from an ECR source (Marti *et al* 2001, Bodendorfer *et al* 2008). Although the FEA prototype was designed to measure electrons, we used a positive argon ion beam to measure the electro-optical response, which should be the same after inverting the potentials since the measurements are carried out with static electric fields. The ion beam is well calibrated and controlled in this facility. The beam energy was controlled by floating the entire ECR source, while leaving the extraction voltage at 3 kV. This method has produced calibrated ion beams with energies down to less than 10 eV.

Figure 3 compares the measured and simulated ESA analyser constant. To determine the azimuthal response of the instrument we used an imaging micro-channel plate (MCP) delay-line detector at the exit of the ESA. The MCP was tested to be in saturation with a bias of 2100 V, and was floated such that the entrance to the MCP was 100 V less than the exit of the analyser. The resulting images show that the azimuthal variation from a point source beam is very similar to the simulated response (figure 4). This detector covered

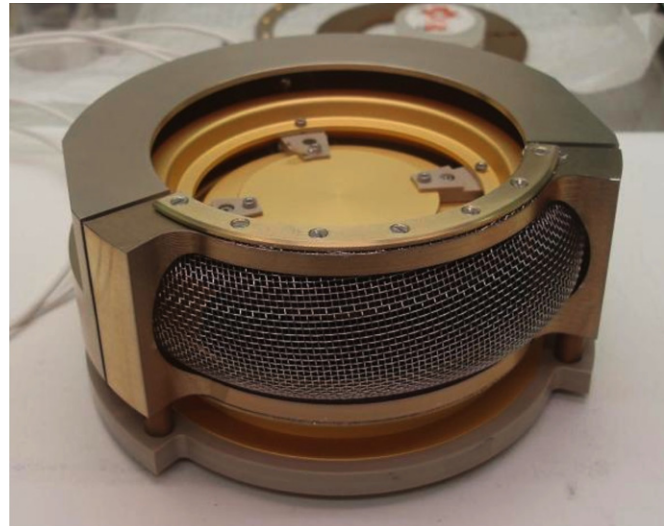


**Figure 2.** Prototype sensor with view on the front grid and the top plate in the centre. The electron/ion-optical elements are the same as for a flight sensor, but only a 90° field of view in azimuth has been realized for simplicity.

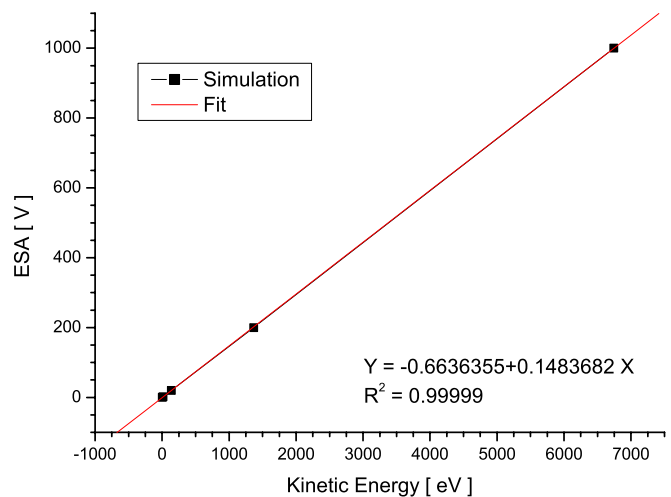


**Figure 3.** Energy analyser constant. The analyser constant as determined by simulation is  $k = 0.148$ . Measurements with the argon beam in the MEFISTO calibration facility yielded an analyser constant  $k = 0.146$ .

only a portion of the exit, adequate to cover the incoming beam direction. A flight model would include a detector that covers the entire ESA exit, enabling measurement over the full range of azimuth angles, with adjusted post-acceleration if measuring electrons.

To determine the elevation response the prototype was mounted on a rotating table, which was moved with respect to the primary ion beam. Elevation control voltages were then applied, showing that the elevation angle response of the instrument was very similar to the simulations (figure 5) as is the energy resolution (figure 6, see also table 2 for a comparison of the simulated and measured performances of the instrument). From the testing we measured the voltages required to select various ranges of energy and elevation

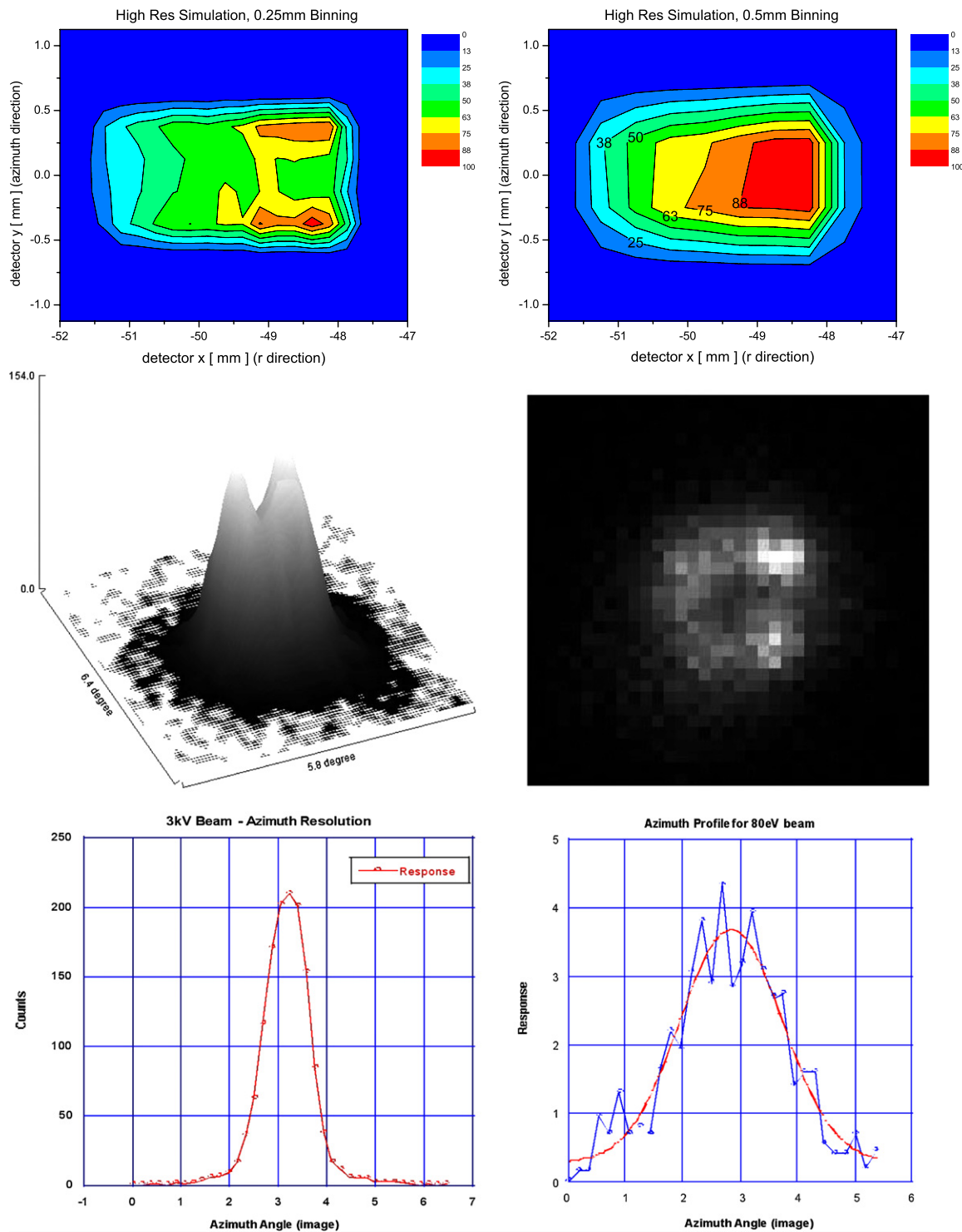


**Figure 4.** Spatial resolution (azimuth)—image on detector. Top left: simulated contour plot of a 3 keV electron beam image on a 0.25 mm pixel size high-resolution imaging detector (0.3° azimuth resolution). Top right: the same for a 0.5 mm pixel size imaging detector (0.6° azimuth resolution). Centre left: measured Ar<sup>+</sup> ion beam image on the delay line detector. Centre right: image of a parallel focused beam on the DLD detector after passage through the analyser, with 40 μm pixel size. It can be seen that the measured response of the prototype verifies the ion optics model. Bottom left: the azimuthal resolution is shown for a 3 kV beam. Bottom right: reduced resolution is seen for lower energy. Standard deviation (*r*) = ± 1.0 mm. Standard deviation (*az*) = ± 0.3 mm: 0.85° azimuth resolution (FWHM).

angles, enabling a scanning procedure to sample the full combination of these in flight.

The geometric factor was controlled by applying voltages to the top plate of the prototype shown in figure 2. The response

is dramatic and once again very similar to the simulations (figure 7). It can be seen here that the geometric factor has been reduced by a factor of 2000 simply by increasing the top-plate voltage and adjusting the elevation voltages accordingly.

**Table 2.** Simulated performances and measured characteristics of the (simplified) prototype and the corresponding flight version.

Parameter	Simulation	Prototype
Particle species	Electrons and ions	Ar <sup>+</sup> ions
Geometric factor (incl. efficiencies)	$(0.02\text{--}2.2) \times 10^{-3} \text{ (cm}^2 \text{ sr eV eV}^{-1}\text{)}$	$(0.022\text{--}2.2) \times 10^{-3} \text{ (cm}^2 \text{ sr eV eV}^{-1}\text{)}$
Spectral range	1 eV–7 keV	5 eV–5 keV
Spectral resolution, $\Delta E/E$	0.064	0.08 (purely ion/electron optics)
Field of view	90° × 360°	90° × 90° (90° × 360° in flight version)
Angular range	4π sr (two instruments)	4π sr with obstructions (two instruments)
Angular resolution	Azimuth: 0.85°  Elevation: 2° at 0°, 4° at 45° (simple mode), 2° (if using all deflection plates)	Azimuth: 1–2° electron/ion optics, 1° anode system; total <3° Elevation: 2° at 0°, 5° at 45° (simple mode)
Temporal resolution	3 s for 3D 0.1 s for 2D (energy–azimuth)	3 s for 3D 0.1 s for 2D (energy–azimuth)

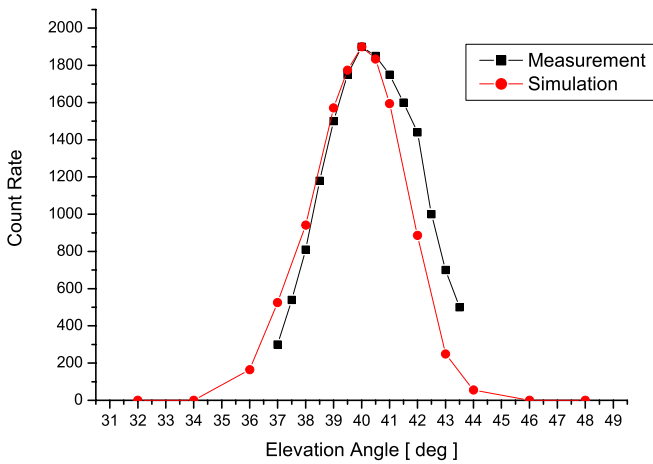


**Figure 5.** Elevation resolution for a nominal 3 keV beam. Elevation angle scan peak width is shown: measurement = 5.0° FWHM at 40.3° (standard deviation = ±2.1°); simulation = 3.9° FWHM at 40.0° (standard deviation = ±1.7°). Measured azimuth resolution at 0° elevation is also shown to be <2°(requirement).

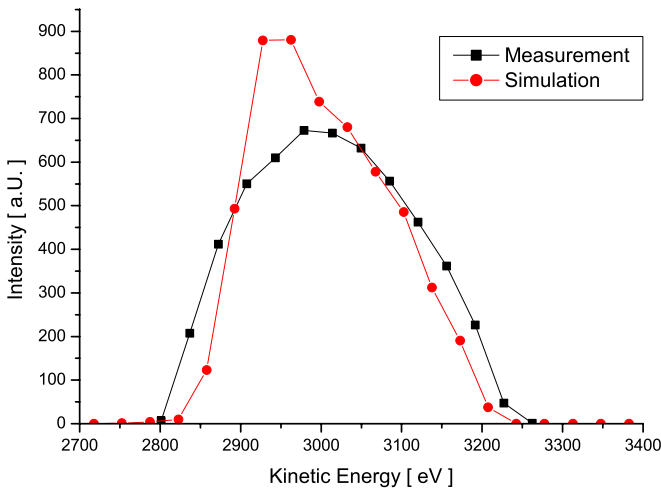


**Figure 6.** Energy resolution. Kinetic energy = 3004 ± 82 eV:  $\Delta E/E = 0.064$  (FWHM) simulated and  $\Delta E/E = 0.08$  (FWHM) measured.

For missions that sample plasmas over many decades in flux, this capability can bring vast improvements in science return.

### 4. Operations

In addition to the controllable geometric factor of the plasma instrument described here, we also emphasize that a FEA-type instrument, when mounted in pairs on opposite sides of a spacecraft, can operate to rapidly measure the full 3D plasma distribution with adequate resolution and desirable electronic control capabilities. The three dimensions in the instrument coordinates are energy, elevation and azimuth. Although we have not performed a full instrument calibration for flight, we demonstrated the voltage response and resolution both in simulation and in measurements with the prototype. The focusing and limiting effect of the top-plate voltage can increase the angular and energy resolution of the instrument when measuring high fluxes, while the elevation and energy control voltages scale linearly to allow a sweeping operation mode (figure 8).

The FEA has the sensitivity and dynamic range to measure two-dimensional distributions (energy and azimuth angle), in 0.1 s at 20  $R_S$  without saturating the detectors all the way into perihelion. To accommodate the large dynamic range simultaneously with the fast cadence of energy scans we implemented a variable geometric factor by adjusting the voltages on the individual electrodes of the top-hat analyser such that at the lowest energies the geometric factor is reduced by a factor of at least 2000. Figure 7 shows the experimental results from the FEA prototype. Maximal transmission (nominal geometric factor, GF) is selected with the top-plate voltage being zero. By increasing the top-plate voltage, the transmission is reduced. At the same time, the energy resolution  $E/\Delta E$  of the analyser is increased as well. Together, these two effects allow for a reliable adjustment of the geometric factor over more than three decades.

The measurement of the azimuth angle of an incoming particle is the simplest dimension for this instrument because it does not rely on a deflection electrode but on the arrival position on the detector. The azimuth angle is measured instantaneously for each particle by the delay-line anode system while the elevation angle is scanned using the deflection plates. Figure 4 shows prototype results for the angular resolution in azimuth angle using a commercial delay line detector. Since the commercial delay line detector has 40 μm spatial resolution the measured resolution represents

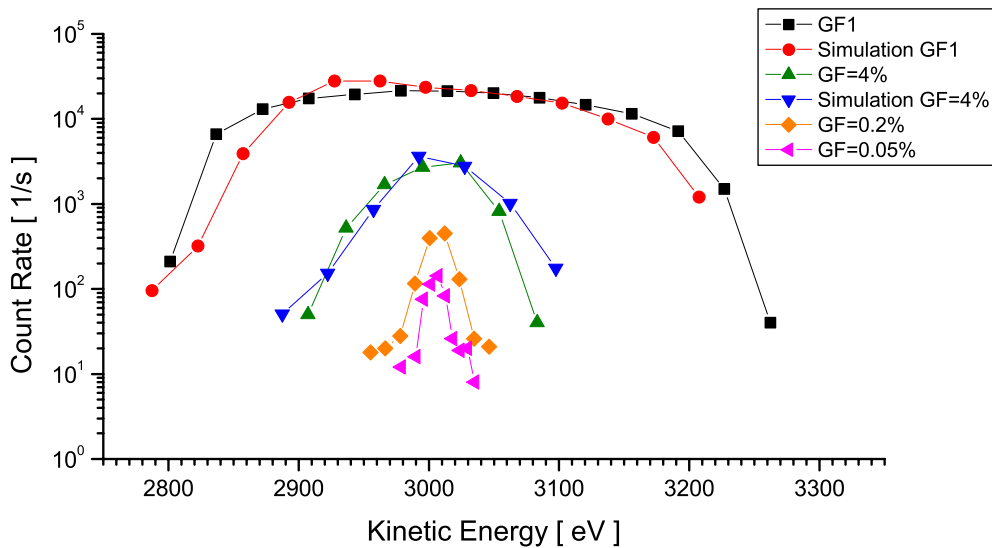


**Figure 7.** Variable geometric factor. Measured and simulated energy resolutions for different geometric factors GF. The geometric factor is adjusted with the top-plate voltage. It can also be seen that the energy resolution increases with decreasing GF.

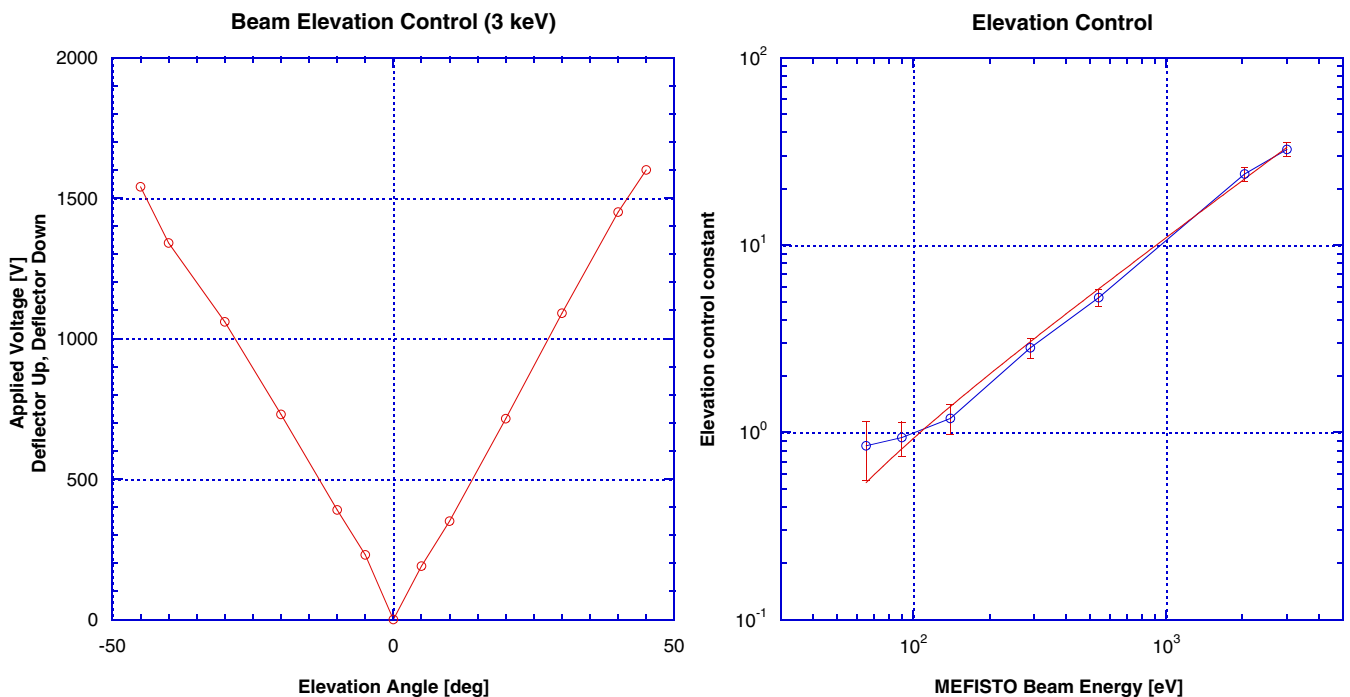


**Figure 8.** Linear response of elevation control voltage. On the left is shown the applied voltage required to observe a given elevation angle, showing the near linear response. The slope of this line is the elevation control constant, which was also measured to behave linearly with energy (right).

the capabilities of the electro-optical system. The measured azimuth angle resolution is between  $1.1^\circ$  and  $2.2^\circ$  depending on energy.

Figure 5 shows prototype results of the angular resolution in elevation angle from simulation and from measurement. The resolution varies somewhat with energy and with the elevation angle, being the highest for high-energy particles at zero elevation. However, the resolution in elevation angle is also improved when operating in reduced geometric factor mode. Figure 8 shows that the control voltage and elevation

control are constant, with linear responses in both elevation and in energy.

By scaling the Lin *et al* (1996) electron measurements from 1 AU to  $9.5 R_S$ ,  $20 R_S$  and  $55 R_S$  we calculated the expected count rates to be recorded by the delay line detector system. These results are shown in table 3 for selected energy steps. Expected counts are given per energy step (of a 0.1 s energy scan) and expressed in count rate per second (Hz). Based on a maximum count rate of 1 MHz for the detector system of the flight instrument we expect nominal performance for recording a 0.1 s energy spectrum (i.e., 2D

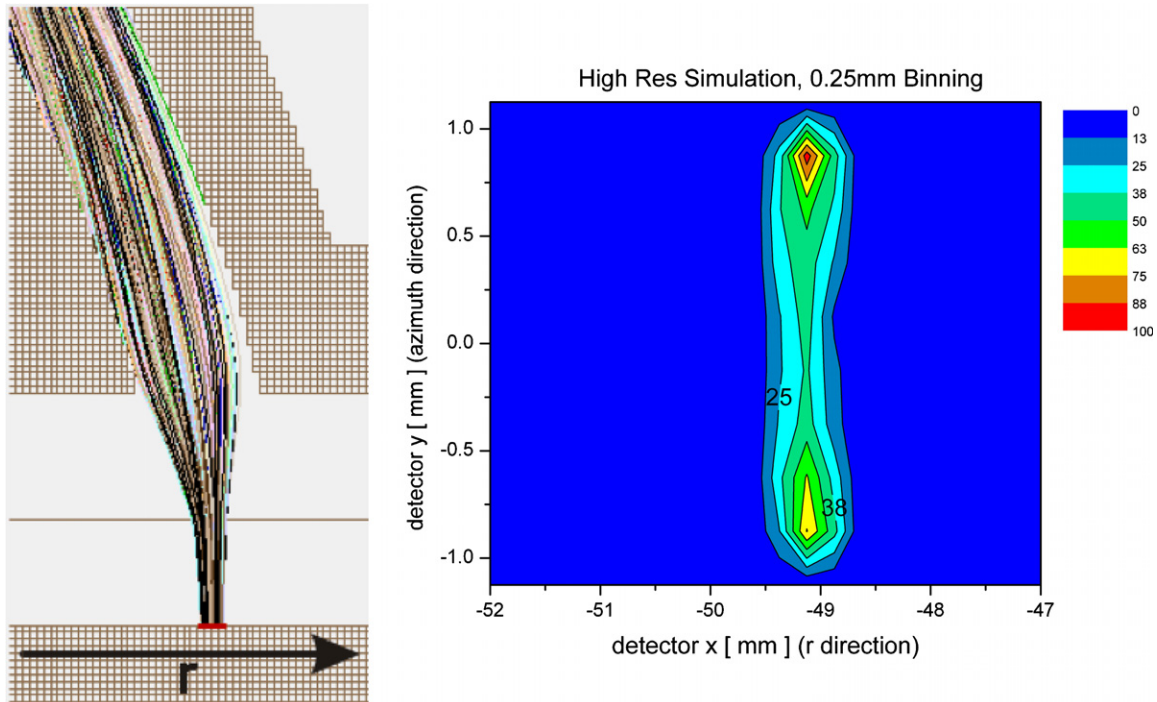


**Figure 9.** Radial (de)focusing for low energy electrons. High-intensity signals (at given energy) can be spread out in  $r$  to increase the detector lifetime; low-intensity signals can be focused in  $r$  to improve S/N. This works for electron energies smaller than the post-acceleration voltage. The azimuthal resolution decreases slightly. The image on the left shows simulated electron trajectories, on the right their simulated image on the detector (compare with figure 4).

**Table 3.** FEA estimated count rates. *Italic font* indicates that the expected count rates allow recording energy spectra during 0.1 s. **Bold font** indicates that the expected count rates are too high to be handled by the detector system. For other entries, integrations longer than 0.1 s are needed to record statistically significant data.

Energy (eV)	$55 R_S$ Counts per E-step	$55 R_S$ Counts per sec.	$20 R_S$ Counts per E-step	$20 R_S$ Counts per sec.	$9.5 R_S$ Counts per E-step	$9.5 R_S$ Counts per sec.
1	<i>1240</i>	$9.2 \times 10^5$	<b><math>9.4 \times 10^3</math></b>	<b><math>6.9 \times 10^6</math></b>	<b><math>4.2 \times 10^4</math></b>	<b><math>3.1 \times 10^7</math></b>
3	<i>240</i>	$1.78 \times 10^5$	<b>1830</b>	<b><math>1.4 \times 10^6</math></b>	<b><math>8.1 \times 10^3</math></b>	<b><math>6.0 \times 10^6</math></b>
10	<i>39</i>	$2.8 \times 10^4$	290	$2.1 \times 10^5$	$1.3 \times 10^3$	$9.5 \times 10^5$
30	<i>7.5</i>	5520	57	$4.18 \times 10^4$	250	$1.85 \times 10^5$
100	<i>1.2</i>	880	9	$6.6 \times 10^3$	40	$2.9 \times 10^4$
300	0.2	170	1.8	1290	7.8	$5.7 \times 10^3$
1000	0.04	27	0.28	205	1.2	910
3000	0.007	5.3	0.05	40	0.24	180
5000	0.003	0.23	0.025	18	0.1	78

distribution function) over most of the energy range (indicated by italic font). Near the Sun, at electron energies  $< 10$  eV the expected count rate would be in excess of the detector capabilities (indicated by bold font in table 3); very high rate times can be at least partially managed through the intrinsic defocusing of intense electron beams on the detector (figure 9) by setting the exit grid to a small deceleration voltage, causing defocussing of the particle beam mainly in the radial direction and therefore reducing the number of particles per unit area reaching the MCP. For safety, stepping of the energy from higher energies to lower energies can be stopped in case where a critical count rate level is reached. Also, near the pericentre of the orbit the energy scan table could be adjusted

to avoid stepping to the lowest energies. The energy range below 10 eV will likely be contaminated by photoelectrons in any case.

The energy resolution of the electro-optical portion alone is  $\Delta E/E = 0.08$  (a result from the FEA prototype characterization) for static operation. Because of the fast energy sweep the energy resolution is reduced to  $\Delta E/E = 0.1$  during normal operation. This energy resolution will be sufficient to resolve the hot electron distributions. However, the energy resolution improves with lower geometric factor operation (figure 7). This means that in addition to a variable geometric factor, the FEA design allows an adjustable energy resolution. If particle fluxes are high enough to yield suitable

statistics a higher energy resolution mode could be employed (which then requires an adjustment of the energy-scan step size or number if coverage of the full energy range is desired). The intrinsic angular resolution of the FEA units is  $3^\circ$  or better for both angles, which allows resolving potentially very narrow halo electron beams (the strahl). Since this high angular resolution is only needed for specific measurements the angular data can be rebinned to a lower resolution most of the time to stay within a reasonable telemetry allocation. In operation, we proposed that the instrument would step in energy and in each energy step scan the elevation. However, due to the linear response of the voltages a suitable scanning mode was found to adequately and safely sample solar electrons from  $9.5 R_S$  to  $55 R_S$ .

## 5. Conclusions

We have demonstrated a compact, relatively simple single-entrance plasma particle instrument capable of variable geometric factor operation, with the GF able to operate with at least a 2000-fold reduction. The operation of this detector requires only voltage changes to control the geometric factor, as well as to scan in elevation and azimuth over  $2\pi$  sr and over three decades in energy. Two such detectors mounted on opposite sides of a spacecraft would be capable of measuring the full 3D velocity distributions of charged particles with high time resolution and over a much higher dynamic range than has previously been demonstrated.

## Acknowledgments

We thank Dr Daniele Piazza and Martin-Diego Busch of the engineering department for their great construction work. We also thank the mechanics workshop for building the prototype, and Georg Bodmer with the Mefisto calibration facility for all their help. This work was supported by the Swiss National Science Foundation.

## References

- Bame S J, Asbridge J R, Felthaus H E, Hones E W and Strong I B 1967 Characteristics of the plasma sheet in the Earth's magnetotail *J. Geophys. Res.* **72** 113–29
- Bodendorfer M, Altwegg K, Shea H and Wurz P 2008 Field structure and electron life times in the MEFISTO Electron Cyclotron Resonance Ion Source *Nucl. Instrum. Method Phys. Res. B* **266** 820–8
- Carlson C W, Curtis D W, Paschmann G and Michael W 1983 An instrument for rapidly measuring plasma distribution functions with high resolution *Adv. Space Res.* **2** 67–70
- Collinson G A and Kataria D O 2010 On variable geometric factor systems for top-hat electrostatic space plasma analyzers *Meas. Sci. Technol.* **21** 105903
- Galvin A B *et al* 2008 The plasma and suprathermal ion composition (PLASTIC) investigation on the STEREO observatories *Space Sci. Rev.* **136** 437–86
- Lin R P *et al* 1995 A three-dimensional plasma and energetic particle investigation for the wind spacecraft *Space Sci. Rev.* **71** 125–53
- Lin R P *et al* 1996 Observation of an impulsive solar electron event extending down to  $\sim 0.5$  keV energy *Geophys. Res. Lett.* **23** 1211–4
- Marti A, Schletti R, Wurz P and Bochsler P 2001 Calibration facility for solar wind plasma instruments *Rev. Sci. Instrum.* **72** 1354–60
- McComas D J *et al* 2007 Understanding coronal heating and solar wind acceleration: case for in situ near-sun measurements *Rev. Geophys.* **45** RG1004
- McComas D J *et al* 2008 Solar probe plus: report of the science and technology definition team, national aeronautics and space administration NASA/TM-2008-214161 (Greenbelt, MD: Goddard Space Flight Center)
- Rème H *et al* 1997 The CLUSTER ion spectrometry (CIS) experiment *Space Sci. Rev.* **79** 303–50
- Rohner U, Whitby J, Wurz P and Barabash U 2004 A highly miniaturised laser ablation time-of-flight mass spectrometer for planetary rover *Rev. Sci. Instrum.* **75** 1314–22
- Sauvaud J-A *et al* 2008 The IMPACT solar wind electron analyzer (SWEA) *Space Sci. Rev.* **136** 227–39
- Sauvaud J-A *et al* 2010 The mercury electron analyzers for the BepiColombo mission *Adv. Space Res.* **46** 1139–48
- Wurz P, Balogh A, Coffey V, Dichter B K, Kasprzak W T, Lazarus A J, Lennartsson W and McFadden J P 2007 Calibration techniques *Calibration of Particle Instruments in Space Physics* ed M Wüest, D S Evans and R von Steiger (ISSI Scientific Report, SR-007) (ESA Communications) pp 117–276